

Nitrogen components in IAB/IIICD iron meteorites

K. V. PONGANIS and K. MARTI*

Department of Chemistry and Biochemistry, University of California at San Diego, La Jolla, California 92093–0317, USA

*Corresponding author. E-mail: kmarti@ucsd.edu

(Received 23 May 2006; revision accepted 17 December 2006)

Abstract—Isotopic variations have been reported for many elements in iron meteorites, with distinct N signatures found in the metal and graphite of IAB irons. In this study, a dozen IAB/IIICD iron meteorites (see Table 1 for new classifications) were analyzed by stepwise pyrolysis to resolve nitrogen components. Although isotopic heterogeneity has been presumed to be lost in thermally processed parent objects, the high-resolution nitrogen isotopic data indicate otherwise. At least one reservoir has a light nitrogen signature, $\delta^{15}\text{N} = -(74 \pm 2)\text{‰}$, at 900 °C to 1000 °C, with a possible second, even lighter, reservoir in Copiapo ($\delta^{15}\text{N} \leq -82\text{‰}$). These releases are consistent with metal nitride decomposition or low-temperature metal phase changes. Heavier nitrogen reservoirs are observed in steps ≤ 700 °C and at 1200 °C to 1400 °C. The latter release has a $\delta^{15}\text{N}$ signature with a limit of $\geq -16\text{‰}$. Xenon isotopic signatures are sensitive indicators for the presence of inclusions because of the very low abundances of Xe in metal. The combined high-temperature release shows ^{131}Xe and ^{129}Xe excesses to be consistent with shifts expected for $\text{Te}(n,\gamma)$ reaction in troilite by epithermal neutrons, but there are also possible alterations in the isotopic ratios likely due to extinct ^{129}I and cosmic-ray spallation.

The IAB/IIICD iron data imply that at least one light N component survived the formation processes of iron parent objects which only partially exchanged nitrogen between phases. Preservation of separate N reservoirs conflicts with neither the model of impact-heating effects for these meteorites nor reported age differences between metal and silicates.

INTRODUCTION

The mechanisms and timing of metal segregation in the early solar system have recently received considerable attention (e.g., Kleine et al. 2005; Maskowski et al. 2006). Isotopic heterogeneity was presumed to be lost in thermally processed parent objects, but the isotopic data show a different picture. El Goresy et al. (1995) showed that isotopically heterogeneous graphite could survive even in a differentiated meteorite. Isotopic compositions of the metal phases and the inclusions of silicates, troilite, chromites, and graphites in some iron meteorites have been shown to be out of equilibrium (Murty and Marti 1994; Zipfel et al. 1996). Zipfel et al. (1996) demonstrated N isotope disequilibrium among co-existing phases in the El Taco (IAB) meteorite. Not only were a variety of graphite morphologies found to have distinct N signatures, but these were also different from those found in silicates and metal.

Iron meteorite ages and the time of metal segregation are older than previously thought. The ^{182}W isotopic variations give information on chronology based on extinct ^{182}Hf

(Horan et al. 1998; Kleine et al. 2005; Markowski et al. 2006; Quitté and Birck 2004), although some inconsistencies in the conclusions remain because ^{182}W isotopic data may be affected by cosmic-ray interactions. Based on limited numbers of measurements, Markowski et al. (2006) propose that ^{182}W in the nonmagmatic IIICD irons might also be consistent with CAIs of Allende, while signatures in IAB and IIE irons may be slightly evolved, although still primitive. These results imply a very early differentiation of metal and silicates in the solar nebula. Other isotopic data are consistent with an early segregation age for the metal and silicates of iron meteorites. Based on the ^{39}Ar – ^{40}Ar age of 4.50–4.54 Gyr for Caddo County (Takeda et al. 2000), the age of the parent object is close to the canonical ages of small parent bodies and also implies a very early segregation of metal and silicate. Bogard et al. (2005) report additional ^{39}Ar – ^{40}Ar ages from silicates of three different Caddo County samples, consistent with a common age of 4.50–4.51 Gyr. Age differences between the metal and silicate phases of IAB iron meteorites were recently reported by Schultz et al. (2006).

The cooling rates of iron meteorites can be determined by matching the calculated Ni composition profiles in taenite obtained from computer simulations with measured profiles in meteoritic taenite and kamacite (e.g., Goldstein and Ogilvie 1965). Hopfe and Goldstein (2001) applied this technique to the IAB irons Toluca and Canyon Diablo using simulated linear cooling rates. They concluded that general shapes are frozen at ~ 450 °C and obtained cooling rates for Toluca taenite (25–100 °C/Myr) and for kamacite (10–30 °C/Myr), while the Ni profile of Canyon Diablo kamacite was modeled using 20–100 °C/Myr cooling rates. Herpfer et al. (1994) suggested that silicates and metal of several IAB meteorites cooled at rates of 30–70 °C per Myr from an assumed peak silicate temperature of ~ 1470 K about 4.565 Gyr ago. These authors concluded that the ^{39}Ar - ^{40}Ar ages of Niemeyer (1979a) (after revision by a factor of 0.988 to correct for the age of the St. Severin irradiation monitor used in his work) were too young to be consistent with the large metal-derived cooling rates. They offered two explanations for the discrepancy: either the maximum metamorphic temperature was achieved more recently or the parent body was covered by an insulating regolith.

The relatively high abundance of silicates in the IAB group suggests that metal segregation was less efficient than in magmatic iron groups. The silicates contain primitive noble gas inventories. Several proposals have been advanced to explain the formation of this group. They include the fractional crystallization of a magma source (Benedix et al. 2005), a series of extractions from the partial melts of a chondritic parent body (Kelly and Larimer 1977), and the impact melting of a porous, chondritic object (Choi et al. 1995). Wasson and Kallemeyn (2002) have divided the two groups IAB and IIICD into five subgroups (see Table 1) and numerous, closely related grouplets using their Au, Ga, Co, and Ni abundance data and suggest that the close compositional relationships between the main IAB group and low-Au subgroups are the result of independent impact events occurring at separate locations on the same parent body. Nitrogen is an important element to constrain formation conditions since it is involved in both nebular and parent body processes. It is particularly important in iron meteorites because of its abundance in the metal matrix, which is unlike other important light elements, such as oxygen, carbon, and hydrogen.

Distinct nitrogen signatures between groups of irons are now well established. Prombo and Clayton (1993) and Franchi et al. (1993) used one-step extractions of the bulk metal and reported averages of distinct signatures. Bulk extraction has a limitation if there is more than one N reservoir present in the metal samples. Even clean, small metal pieces may harbor inclusions beneath the surface and some may be particularly N-rich. This is particularly important if combustion is used to extract N from a metal, since oxidation of the metal tends to smear out the release and may obscure multicomponent releases. Many of the inclusions found in IAB/IIICD

meteorites carry significant amounts of nitrogen with distinct $\delta^{15}\text{N}$ signatures. Work by Zipfel et al. (1996) showed that the silicates in El Taco (IAB) contained a much heavier signature than the metal, as did most of the graphites. In contrast, Franchi et al. (1993) studied acid residues consisting of minor phases of IAB and other irons using stepped combustion and found N isotopic ratios close to the bulk values for these meteorites. Prombo and Clayton (1993) measured very light nitrogen ($\delta^{15}\text{N} = -73.2\text{‰}$) from the troilite of Canyon Diablo. Nitrides can be present in iron meteorites, as Buchwald and Scott (1971) reported the presence of carlsbergite in iron meteorites. Nielsen and Buchwald (1981) also reported the presence of roaldite in Toluca. Sugiura (1998) reported tiny areas with abundant CN^- in a taenite phase of Toluca, which he suggested might be due to the presence of roaldite, although he did not report $\delta^{15}\text{N}$ for these inclusions.

EXPERIMENTAL PROCEDURES

In this study, seventeen samples of a dozen IAB/IIICD (for new group assignments see Table 1) meteorites were selected and analyzed for N concentration and isotopic signatures by stepwise pyrolysis. Samples were inspected under a binocular microscope and material was taken from regions with no visible inclusions on the surface. Meteorites were either cut using stainless-steel tools (nippers and hacksaw) or sliced using a wire saw. Most samples were in the 20 to 50 mg range. Although the selected samples were chipped or sliced from clean matrix metal, inclusions may have existed below the surface. Samples were pre-outgassed at 150 °C for up to 12 h to remove absorbed terrestrial contamination. Gases were released by stepwise pyrolysis in a resistance quartz furnace, which was used in steps up to 1000 °C and 1050 °C. Samples were transferred in vacuo into an Mo-crucible and heated by radio frequency for extraction steps at temperatures >1050 °C. The experimental approach follows that discussed by Mathew et al. (2005), except where indicated. Nitrogen was continuously adsorbed on zeolite at liquid nitrogen temperature during the extraction to minimize gettering by the extraction system and crucible. The recovery of sample N_2 by this technique was calibrated to be $80 \pm 5\%$ and no isotopic variations were observed for air standard pipettes. The mass spectra were taken by peak jumping using a magnetic field controller. The mass 30 peak was measured to correct for CO interferences and for mass discrimination using the operational procedures discussed by Mathew et al. (2005). The mass spectrometer sensitivity for N as judged from air pipettes was constant within 5%. Xe was analyzed to monitor for the presence of inclusions. Since the presence of silicates, graphite, or troilite in the metal matrix can potentially alter the N signature, the Xe signature is a useful monitor for inclusions. Xe was condensed in a glass finger at the temperature of liquid N_2 and analyzed after the nitrogen. The analytical procedures for xenon follow those given by Mathew et al. (2000).

Table 1. The N release for the 17 IAB/IIICD samples of metal matrix by stepwise pyrolysis. New group assignments (Wasson and Kallemeyn 2002) are given in parentheses.

Meteorite	Extraction temperature (°C)	N (ppm)	$\delta^{15}\text{N}^{\text{a}}$ (‰)	CR total $\delta^{15}\text{N}^{\text{b}}$ (‰)
Balfour Downs 1, IAB (Group: IAB-sLL)	500	–	–	
	700	2.03	-37.9 ± 3.3	
	900	2.94	-51.9 ± 2.3	
	1000	12.55	-56.8 ± 5.1	
	1200	3.34	-53.0 ± 1.3	
	1400	5.32	-53.3 ± 1.7	
	1550	1.15	-57.0 ± 3.9	
	1600	0.71	-61.0 ± 5.6	
	Total	28.04	-53.9 ± 3.4	-54.2 ± 3.5
	Balfour Downs 2	500	1.19	24.2 ± 5.9
700		1.03	14.5 ± 6.7	
900		0.62	-28.5 ± 4.6	
1000		7.53	-32.1 ± 2.7	
1200		33.21	-32.1 ± 5.2	
1400		26.75	-18.2 ± 2.3	
1550		4.43	-24.7 ± 2.4	
1600		1.44	-26.3 ± 5.1	
Total		74.99	-25.9 ± 3.6	-26.1 ± 3.6
Bischtübe 1, IAB (Group: IAB-sLL)	500	0.69	31.3 ± 4.3	
	700	0.80	18.7 ± 4.9	
	900	0.80	18.7 ± 4.9	
	1000	4.49	-47.4 ± 1.6	
	1200	29.38	-32.6 ± 3.4	
	1400	9.27	-22.7 ± 1.8	
	1550	2.84	-40.8 ± 1.7	
	1600	0.84	-28.4 ± 4.8	
	Total	48.41	-31.4 ± 2.5	-31.5 ± 2.5
Bischtübe 2	500	0.48	32.1 ± 6.5	
	700	2.57	-61.1 ± 2.8	
	900	2.05	-59.8 ± 3.9	
	1000	10.54	-62.2 ± 3.3	
	1200	12.05	-52.9 ± 1.9	
	1400	8.48	-33.2 ± 2.2	
	1550	1.41	-33.0 ± 5.4	
	1600	0.76	-32.8 ± 5.2	
	Total	37.86	-50.8 ± 2.5	-50.9 ± 2.5
Carlton, IIICD (Group: IAB-sLM)	500	0.04	-2 ± 16	
	700	1.34	-75.0 ± 1.3	
	900	1.14	-69.7 ± 1.8	
	1000	2.62	-72.9 ± 1.8	
	1200	2.59	-67.3 ± 1.5	
	1400	14.14	-50.5 ± 1.0	
	1550	2.12	-64.6 ± 2.1	
	1600	0.54	-65.5 ± 6.6	
	Total	24.49	-58.5 ± 1.0	-58.8 ± 1.0
Copiapo 1, IAB (Group: IAB-MG)	500	0.06	11.4 ± 12.3	
	700	0.11	-7.5 ± 9.1	
	900	6.61	-71.5 ± 2.6	
	1000	9.24	-70.3 ± 1.8	
	1200	18.68	-70.6 ± 3.5	

Table 1. *Continued.* The N release for the 17 IAB/IIICD samples of metal matrix by stepwise pyrolysis. New group assignments (Wasson and Kallemeyn 2002) are given in parentheses.

Meteorite	Extraction temperature (°C)	N (ppm)	$\delta^{15}\text{N}^{\text{a}}$ (‰)	CR total $\delta^{15}\text{N}^{\text{b}}$ (‰)
	1400	3.24	-47.8 ± 3.6	
	1550	0.94	-64.3 ± 4.0	
	1600	0.30	-62.5 ± 5.6	
	Total	39.12	-68.4 ± 2.7	-68.4 ± 2.7
Copiapo 2	500	0.19	18.3 ± 8.0	
	700	0.17	-23.8 ± 4.7	
	900	17.14	-82.4 ± 2.0	
	920	10.13	-78.0 ± 3.4	
	940	8.08	-78.3 ± 1.6	
	960	4.45	-75.0 ± 1.9	
	980	11.46	-78.6 ± 3.7	
	1000	13.53	-73.5 ± 3.0	
	1050	14.95	-75.0 ± 1.7	
	1100	1.82	-51.4 ± 5.4	
	1200	9.76	-60.1 ± 2.3	
	1300	7.57	-55.4 ± 3.3	
	1400	1.79	-49.5 ± 2.2	
	1550	1.66	-56.9 ± 3.5	
	1600	0.44	-67.9 ± 10.3	
Total	102.94	-72.9 ± 2.3	-72.9 ± 2.3	
Dayton, IIICD (Group: IAB-sLH)	500	–	–	
	700	0.94	-9.7 ± 2.4	
	900	0.89	-44.9 ± 1.8	
	1000	4.65	-70.8 ± 1.6	
	1200	0.90	-66.6 ± 1.7	
	1400	7.65	-55.9 ± 1.3	
	1550	0.84	-62.4 ± 2.7	
	1600	0.32	-71.1 ± 7.7	
	1600 2nd time	0.31	-81.2 ± 12.7	
	Total	16.51	-58.6 ± 2.1	-58.7 ± 2.1
Haniet el Beguel, IAB (Group: IAB)	500	0.03	-4.4 ± 46.5	
	700	0.18	-63.6 ± 10.9	
	900	3.98	-68.6 ± 1.9	
	1000	13.52	-70.0 ± 1.8	
	1200	31.93	-52.9 ± 5.1	
	1400	2.13	-44.8 ± 3.5	
	1550	1.69	-65.0 ± 6.3	
	1600	0.67	-63.6 ± 9.1	
	Total	54.10	-58.5 ± 3.7	-58.7 ± 3.7
Hope, IIICD (Group: IAB-MG)	500	1.15	4.4 ± 14.5	
	700	0.59	29.1 ± 8.0	
	900	1.62	-57.1 ± 2.7	
	1000	1.32	-55.8 ± 4.5	
	1200	2.75	-38.3 ± 3.6	
	1400	1.63	-48.4 ± 2.4	
	1550	0.49	-49.4 ± 16.1	
	1600	0.12	-49.5 ± 26.5	
	Total	8.51	-42.6 ± 4.4	-42.6 ± 4.4
Lamesa, IIICD (Group: IAB-sLM)	500	0.69	7.9 ± 12.1	
	700	0.38	-63.3 ± 5.1	
	900	4.23	-76.8 ± 3.3	
	1000	44.44	-72.8 ± 1.9	

Table 1. *Continued.* The N release for the 17 IAB/IIICD samples of metal matrix by stepwise pyrolysis. New group assignments (Wasson and Kallemeyn 2002) are given in parentheses.

Meteorite	Extraction temperature (°C)	N (ppm)	$\delta^{15}\text{N}^a$ (‰)	CR total $\delta^{15}\text{N}^b$ (‰)
	1100	0.18	-33.6 ± 6.9	
	1200	7.40	-44.3 ± 2.2	
	1300	3.59	-26.1 ± 1.4	
	1400	0.41	-31.6 ± 3.9	
	1550	0.75	-32.6 ± 2.5	
	1600	0.25	-34.1 ± 5.6	
	Total	61.63	-65.9 ± 1.6	-65.9 ± 1.6
Odessa 2, IAB (Group: IAB-MG)	RF 900	15.13	-66.6 ± 1.0	
	RF 1200	74.01	-62.4 ± 1.3	
	RF 1400	5.19	-62.2 ± 3.4	
	RF 1550	11.63	-71.0 ± 1.9	
	RF 1600	3.42	-69.1 ± 3.6	
	Total	109.4	-64.1 ± 1.4	-64.1 ± 1.4
Odessa 4	500	1.04	27.8 ± 4.3	
	600	0.44	-18.6 ± 0.8	
	700	0.62	-57.0 ± 1.0	
	800	0.47	-43.7 ± 1.3	
	900	2.65	-73.0 ± 1.0	
	1000	38.55	-73.7 ± 0.8	
	1100	0.53	-69.4 ± 2.5	
	1200	13.50	-68.6 ± 1.2	
	1300	27.77	-59.3 ± 2.4	
	1400	24.24	-58.6 ± 1.1	
	1550	6.19	-62.1 ± 1.2	
	1600	2.01	-62.8 ± 1.4	
	Total	117.0	-65.3 ± 1.2	-65.3 ± 1.2
Odessa 5	500	0.79	24.7 ± 5.4	
	600	0.33	13.6 ± 7.1	
	700	0.27	14.8 ± 5.3	
	800	0.14	10.8 ± 11.6	
	850	0.04	26.8 ± 40.0	
	900	0.07	-28.3 ± 27.2	
	1000	0.67	-8.6 ± 2.0	
	1050	0.87	-12.5 ± 2.7	
	700 combustion	0.04	-19.0 ± 43.8	
	1200	0.69	-9.8 ± 6.0	
	1400	1.96	-15.9 ± 2.9	
	1600	3.03	-19.1 ± 12.9	
	Total	8.11	-12.8 ± 7.8	-12.9 ± 7.8
Sarepta, IAB (Group: IAB-MG)	500	0.10	10.9 ± 21.3	
	700	0.29	-16.4 ± 3.2	
	900	1.20	-49.7 ± 1.5	
	1000	3.66	-69.2 ± 1.1	
	1200	30.22	-58.2 ± 2.7	
	1400	10.88	-50.5 ± 1.0	
	1550	2.74	-64.0 ± 2.8	
	1600	0.89	-67.1 ± 5.1	
	Total	49.87	-57.3 ± 2.1	-57.3 ± 2.1
Tazewell, IIICD (Group: IAB-sLH)	500	0.48	44.5 ± 4.4	
	700	0.65	-49.5 ± 2.3	
	900	1.23	-72.4 ± 1.8	
	1000	6.39	-74.5 ± 2.1	

Table 1. *Continued.* The N release for the 17 IAB/IIICD samples of metal matrix by stepwise pyrolysis. New group assignments (Wasson and Kallemeyn 2002) are given in parentheses.

Meteorite	Extraction temperature (°C)	N (ppm)	$\delta^{15}\text{N}^{\text{a}}$ (‰)	CR total $\delta^{15}\text{N}^{\text{b}}$ (‰)
	1200	2.41	-68.2 ± 1.4	
	1400	15.23	-56.7 ± 1.7	
	1550	1.93	-65.0 ± 1.8	
	1600	0.62	-70.8 ± 5.2	
	1600 #2	0.57	-49.0 ± 2.6	
	Total	29.04	-62.8 ± 1.7	-63.0 ± 1.7
Yardmyly 3, IIICD (Group: IAB)	500	0.54	8.5 ± 11.8	
	700	0.82	0.0 ± 7.5	
	900	0.86	5.1 ± 1.8	
	1000	0.74	10.1 ± 4.6	
	1200	2.55	-13.6 ± 2.1	
	1400	5.31	-15.8 ± 4.2	
	1550	0.84	-5.0 ± 2.8	
	1600	0.26	-9.4 ± 4.5	
	Total	11.37	-10.0 ± 3.7	-10.7 ± 3.9

^aThe total N concentration and signature of each sample is calculated from steps for $500\text{ °C} < T \leq 1600\text{ °C}$. The values are corrected for mass discrimination and CO interference as described by Mathew et al. (2005). Uncertainties in N concentrations are estimated as $\sim 10\%$, based on the reproducibility on N air standard amounts of 5% (Mathew et al. 2005).

^bThe total $\delta^{15}\text{N}$ values are corrected for $^{15}\text{N}_c$ using ^{21}Ne spallation data from Lavielle (personal communication) for all meteorites except Balfour Downs and Bischtübe, where data from Voshage et al. (1979) was used. No corrections for $\delta^{15}\text{N}$ recoils from oxygen in inclusions are done.

RESULTS

The N concentrations and isotopic signatures released in individual temperature steps, along with the total N concentration and signature for $500\text{ °C} < T \leq 1600\text{ °C}$ range, are reported in Table 1. The release patterns are shown in Fig. 1. The step-release plots show that nitrogen isotopic systematics can be complex and that data in the literature based on one-step melting analyses may be misleading. The different nitrogen components need to be identified before these can be assessed regarding origins and incorporation mechanisms. First, we assess spallation $^{15}\text{N}_c$ contributions from cosmic-ray (GCR) reactions to the nitrogen budget of irons. These corrections are small in most cases, since the nitrogen concentrations are generally large. In irons, ^{21}Ne and $^{15}\text{N}_c$ produced from Fe and Ni are made mostly by high-energy GCR particles. The $(^4\text{He}/^{21}\text{Ne})_c$ production ratio increases with shielding depth in any given meteorite, reflecting the build-up of secondary particles. This ratio has been successfully used as a shielding parameter for various iron meteorites. Constant $^{21}\text{Ne}/^{10}\text{Be}$ ratios (Lavielle et al. 1999) as well as a constant $(^{21}\text{Ne}/^{15}\text{N})_c = 0.80$ ratio (Mathew et al. 2000) have been inferred. The small $^{15}\text{N}_c$ corrections are calculated from ^{21}Ne spallation data (Lavielle, personal communication) and corrected in Table 1. However, no corrections for ^{15}N recoils from O in inclusions were applied.

The bulk $\delta^{15}\text{N}$ signature for IAB samples previously reported was in the range of -64.4‰ to -51.6‰ , although

Franchi et al. (1993) reported “anomalous” signatures for two samples of Bischtübe ($\delta^{15}\text{N} = -42.8\text{‰}$ and -42.9‰) and Pepin and Becker (1982) reported bulk $\delta^{15}\text{N}$ values as high as -13.5‰ for Toluca. The samples in Table 1 show a larger range of total $\delta^{15}\text{N}$ values (-72.9‰ to -10.7‰). Replicate total data are also sometimes variable, possibly due to inclusions. This problem is ubiquitous for these irons. Prombo and Clayton (1993) reported $\delta^{15}\text{N}$ values of -68.9‰ , -49.9‰ , and -66.7‰ for Canyon Diablo. Pepin and Becker (1982) reported $\delta^{15}\text{N}$ values of -13.5‰ and -40.9‰ for Toluca. We measured three samples of Odessa with total $\delta^{15}\text{N}$ values of -64.1‰ , -65.3‰ , and -12.8‰ , where the last sample has also a much lower N concentration (Table 1). Similarly, our total N values for the two samples of Balfour Downs (IAB) (-53.9‰ and -25.9‰) and the two samples of Bischtübe (IAB) (-31.4‰ and -50.8‰) do not overlap. Nitrogen in two samples of Copiapo is dominated by a very light N component. In particular, Copiapo 2 has an average signature $\delta^{15}\text{N} \sim -77\text{‰}$ for $700 < T \leq 1050\text{ °C}$; based on the low ^{21}Ne concentration in Copiapo, the N isotope ratio requires no $^{15}\text{N}_c$ correction. A similar release is seen in Copiapo 1, but the temperature resolution of the N release is not as detailed. The small nitrogen release at temperature steps $\leq 500\text{ °C}$ may represent an atmospheric contamination; for temperature steps between 700 °C and 1050 °C , the signature is very light (-82.4‰ to -73.5‰), and this release may also contain more than one reservoir (Table 1; Fig. 1). A much lower N concentration in the 1400 °C step in fact reveals a nitrogen component with $\delta^{15}\text{N} > -48\text{‰}$, which

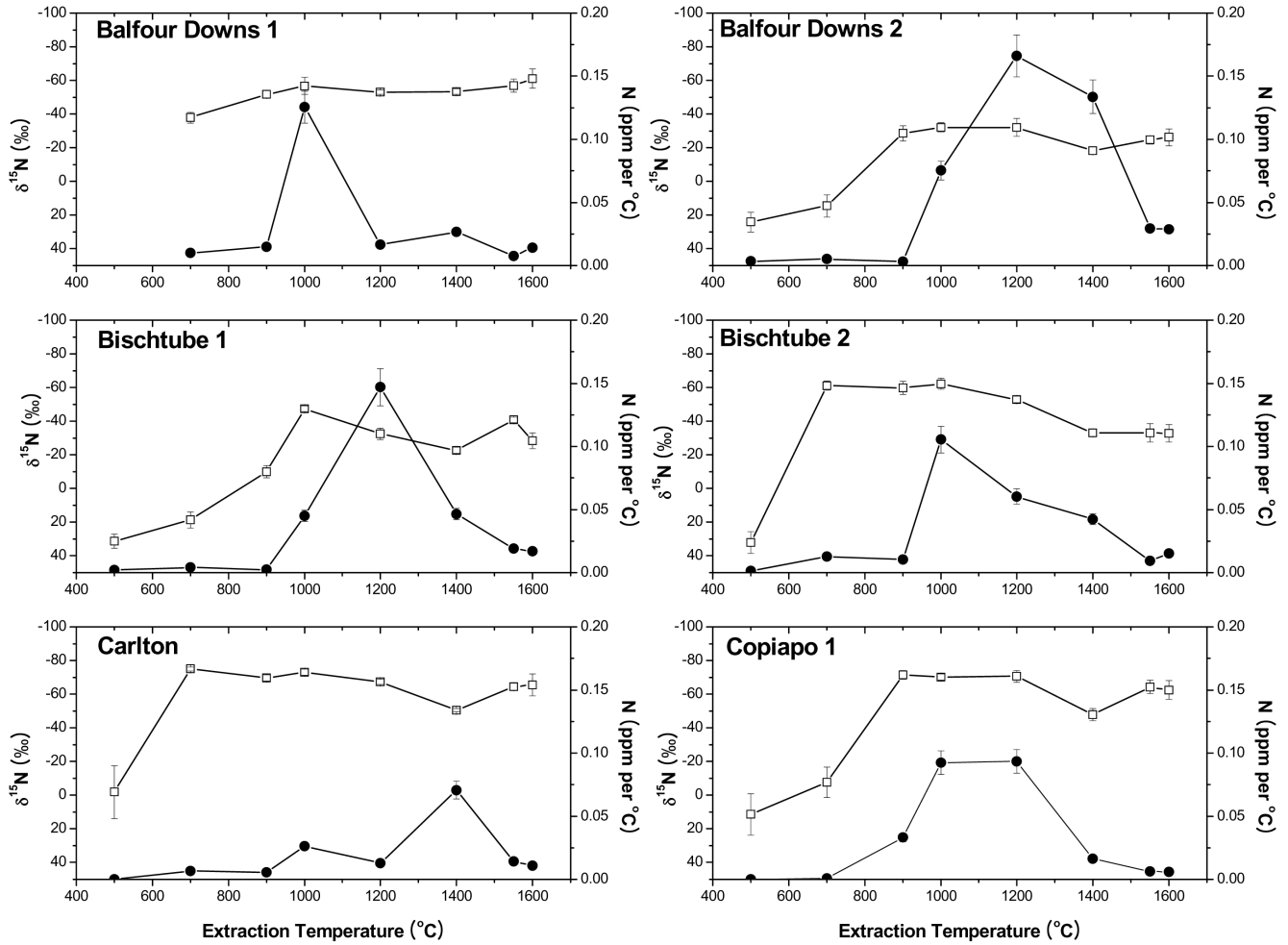


Fig. 1. The N step-release profiles for 17 samples of a dozen IAB irons. Temperature steps are from 500 °C to 1600 °C. The amount of N released has been normalized to ppm per °C. The step release curve for N in Copiapo 2 has the most detail. Copiapo 2 shows two distinct, low-temperature components. The $\delta^{15}\text{N}$ values for these low-temperature reservoirs are approximately the same. Note that the temperature increase after the last quartz furnace step (1050 °C) to the first radio frequency extraction step (1100 °C) (see Table 1) is not certain because different measurements of temperature are used. Therefore, in Copiapo 2 the 1100 °C data was combined with the data of the 1200 °C step.

apparently causes shifts in 1400 °C data and also a minor shift in the melt fraction (1550 °C).

Figure 1 shows that the light nitrogen signature is not restricted to Copiapo. Several other iron samples have very light N components following the 700 °C step. For example, the IAB iron Harriet de Beguel has similar release characteristics to Copiapo, but in this case, the heavy component already appears in the 1200 °C fraction where most of the N is released. Although this release pattern permits us to set a limit of $\delta^{15}\text{N} > -45\text{‰}$ for a heavier N component, we can obtain better constraints for the “heavy” nitrogen reservoir using the release profiles of the Odessa (IAB) and Yardmyly (IIICD). Two of the three Odessa samples are dominated by a very light N component, but Odessa 5, Balfour Downs 2, and Yardmyly 3 possess a heavy N component that has a release at the 1400 °C step, -15.8‰ , -18.2‰ , and -15.9‰ , respectively. The two 1400 °C steps

from Odessa 5 and Yardmyly 3 refine the lower limit for “heavy” N to $\delta^{15}\text{N} \sim -16\text{‰}$.

The two Ni-rich (>10% Ni) IIICD irons Dayton and Tazewell (Fig. 2) show almost identical N release systematics and a constant abundance ratio for the inferred light and heavy N components. These release profiles suggest that two meteorites have a common parent body source, although the $^{21}\text{Ne}_c$ CRE ages and their ejection times are different (Lavielle, personal communication). Based on class, Ni composition, and nitrogen systematics, these two meteorites, and perhaps Carlton (IIICD) as well, seem to form a grouplet. All possess the light N signature of IAB irons. Carlton’s N release pattern is similar to the other two, although its overall total $\delta^{15}\text{N}$ is somewhat heavier. Note that a fourth high-Ni (IIICD) meteorite, Lamesa, has a distinctive N release pattern. Light nitrogen is not only observed in the release around 1000 °C, but also in the melting releases (1600 °C step) for all

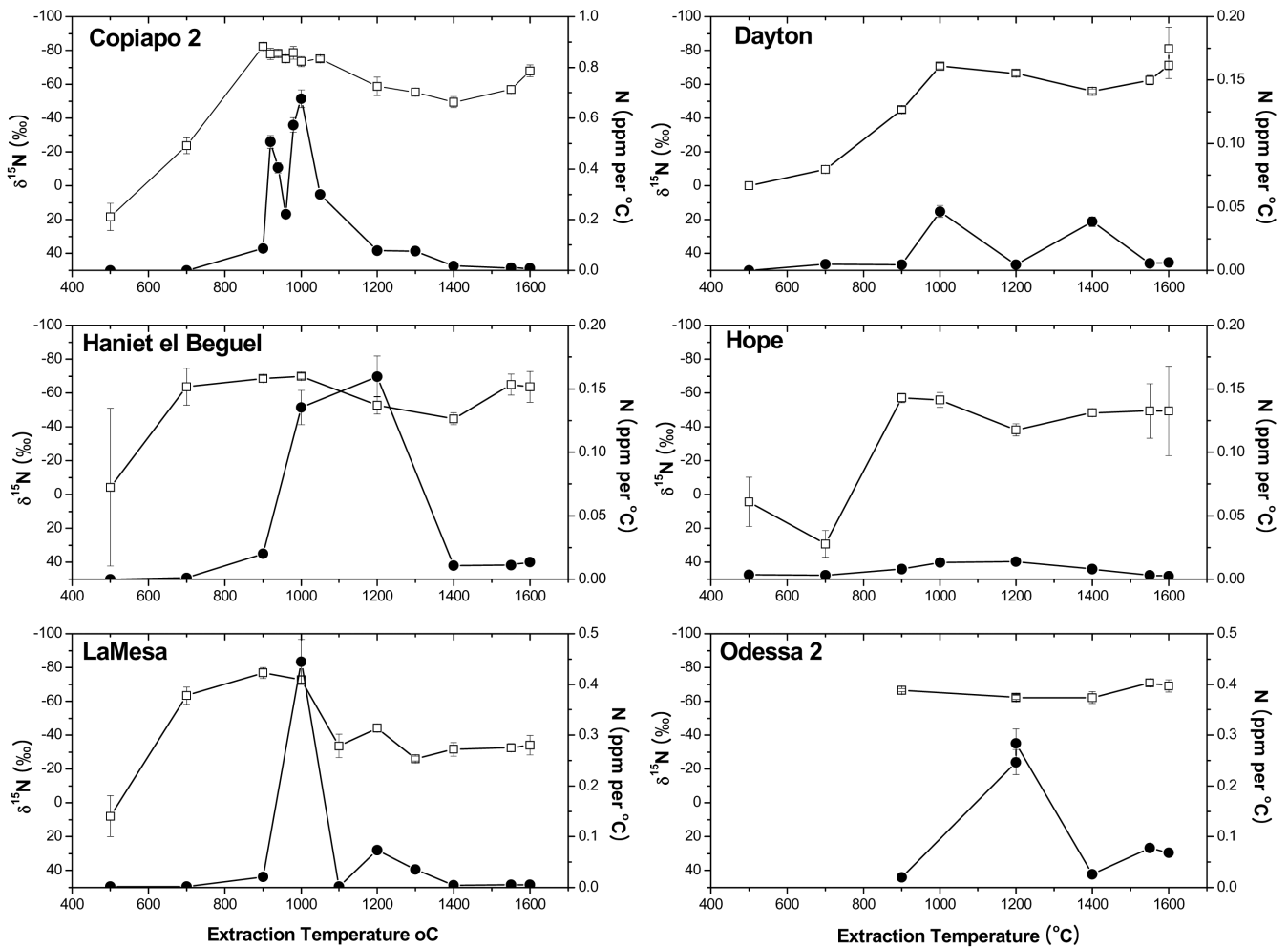


Fig. 1. *Continued.* The N step-release profiles for 17 samples of a dozen IAB irons. Temperature steps are from 500 °C to 1600 °C. The amount of N released has been normalized to ppm per °C. The step release curve for N in Copiapo 2 has the most detail. Copiapo 2 shows two distinct, low-temperature components. The $\delta^{15}\text{N}$ values for these low-temperature reservoirs are approximately the same. Note that the temperature increase after the last quartz furnace step (1050 °C) to the first radio frequency extraction step (1100 °C) (see Table 1) is not certain because different measurements of temperature are used. Therefore, in Copiapo 2 the 1100 °C data was combined with the data of the 1200 °C step.

four, indicating that the heavy N components were depleted first, including a cosmic-ray-spallation component.

Radiogenic and Cosmic Ray Signatures as Monitors of Inclusions in Irons

Noble gas isotopic signatures may act as sensitive indicators for the presence of other minerals because of the very low abundances of indigenous noble gases. We have separated Xe fractions from the N in all temperature steps and analyzed summed fractions for steps ≤ 1000 °C and for steps > 1000 °C because the amounts in individual steps were very low ($< 1.3 \times 10^{-11}$ cm³ STP/g), as expected for clean metal samples. Useful information can be obtained from the most abundant isotopes: ¹²⁹Xe, ¹³¹Xe, and ¹³²Xe (Table 2). Since graphite inclusions carry large concentrations of indigenous Xe (Maruoka et al. 2001), the release characteristics of ¹³²Xe

concentrations might indicate the presence of graphite. Also, multiple isotopic nitrogen signatures in various morphologies of graphite were reported by Zipfel et al. (1996) in the El Taco IAB iron. We added a combustion step in Odessa 5, which did not release significant amounts of either Xe or N. However, the release pattern of Odessa 5 was unlike the other two Odessa samples, so this result only says that this particular sample contained little to no graphite.

The observed xenon isotope ratios are also reported in Table 2. A plot of $\delta^{15}\text{N}$ at 1400 °C plotted versus measured high-temperature ¹²⁹Xe/¹³²Xe ratios (Fig. 3) shows a rough correlation, suggesting the presence of inclusions within the metal matrix that influence the N isotopic signature. On the other hand, with the exception of Odessa, most samples contain rather similar concentrations of ¹³²Xe (Table 1), suggesting that ¹²⁹Xe concentrations may be variable. This possibility is explored in Fig. 4, where low-temperature

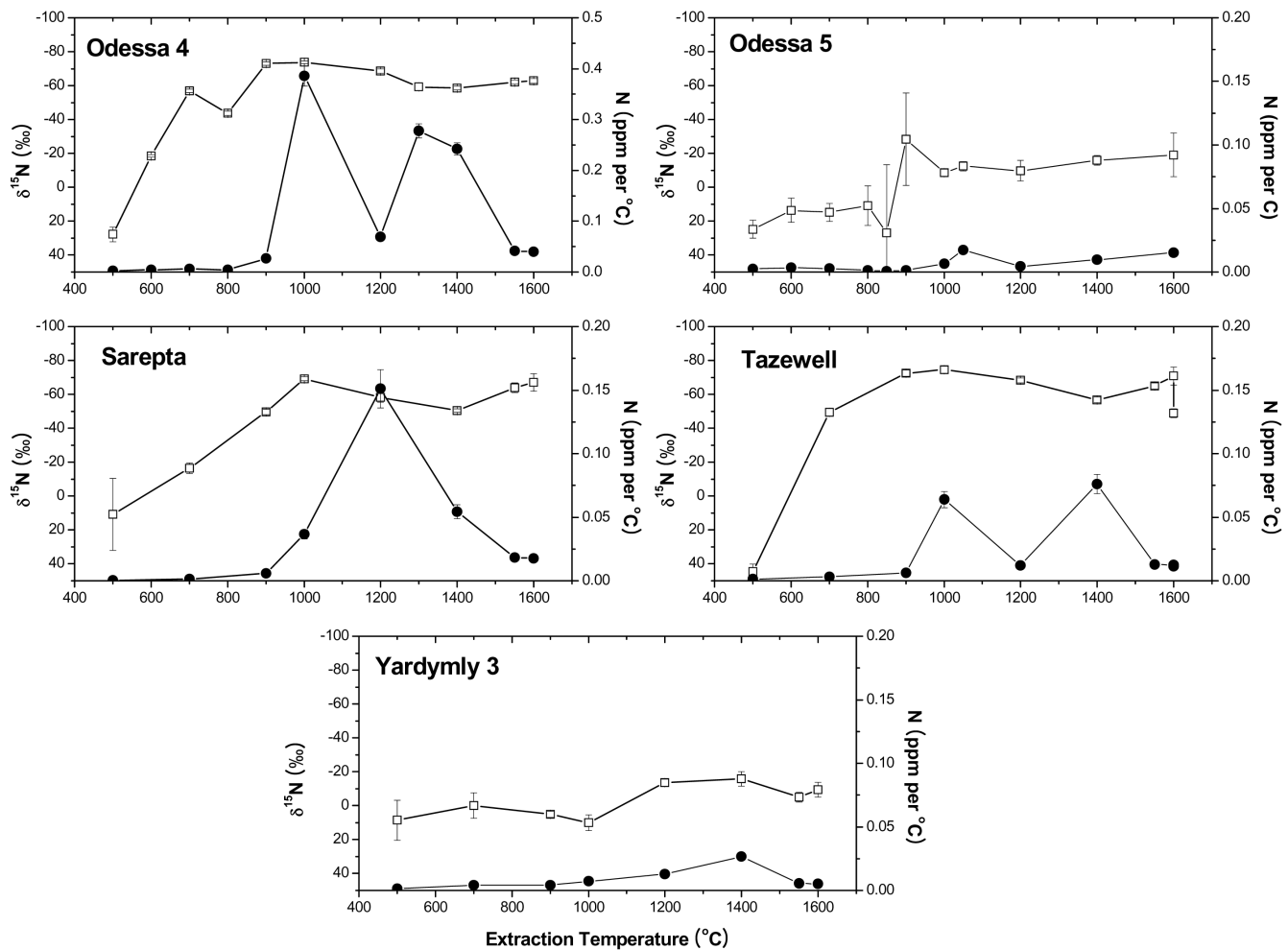


Fig. 1. *Continued.* The N step-release profiles for 17 samples of a dozen IAB irons. Temperature steps are from 500 °C to 1600 °C. The amount of N released has been normalized to ppm per °C. The step release curve for N in Copiapo 2 has the most detail. Copiapo 2 shows two distinct, low-temperature components. The $\delta^{15}\text{N}$ values for these low-temperature reservoirs are approximately the same. Note that the temperature increase after the last quartz furnace step (1050 °C) to the first radio frequency extraction step (1100 °C) (see Table 1) is not certain because different measurements of temperature are used. Therefore, in Copiapo 2 the 1100 °C data was combined with the data of the 1200 °C step.

$^{129}\text{Xe}/^{132}\text{Xe}$ ratios versus $^{131}\text{Xe}/^{132}\text{Xe}$ ratios (Fig. 4a) show shifts consistent with the spallation signature for most of the samples. However, Bischtübe 2, Balfour Downs 2, and Copiapo 2 all lie above the spallation line, and most high-temperature Xe ratios (Fig. 4b) lie between trend lines with a slope of 3.6 and shifts towards spallation Xe. A slope of 3.6 is calculated and observed for reactions of epithermal neutrons on Te, which is enriched in troilite (Murty and Marti 1987). This plot suggests either the presence of variable amounts of troilite inclusions and Te in troilites in our samples and/or variable shielding conditions. Similarly, the three samples (Bischtübe 2, Balfour Downs 2, and Copiapo 2), that lie off the spallation trend line in Fig. 4a might indicate an early release of Xe from a troilite reservoir.

Furthermore, although not clearly indicated, some shifts in Fig. 4 may also be due to small amounts of radiogenic ^{129}Xe , which has been found in silicate inclusions,

specifically in diopside and albite (Meshik et al. 2004). Meshik et al. (2004) suggested that the excess ^{129}Xe might also be found in the small graphite inclusions around the silicate rims. Trapped Xe was found in graphites (Mathew and Begemann 1995) and graphite inclusions of an IAB iron show concentrations of indigenous Xe, which exceed those in bulk samples by factors of 30 (Maruoka et al. 2001).

DISCUSSION

The possible relationship between irons of groups IAB and IIICD has been controversial, as some investigators have suggested that these two groups represent samples from either different parent bodies or different evolutionary processes (Wasson and Kallemeyn 2002). Although statistics are limited, we show the nitrogen data separately as concentration-weighted averages for the two groups (Fig. 5)

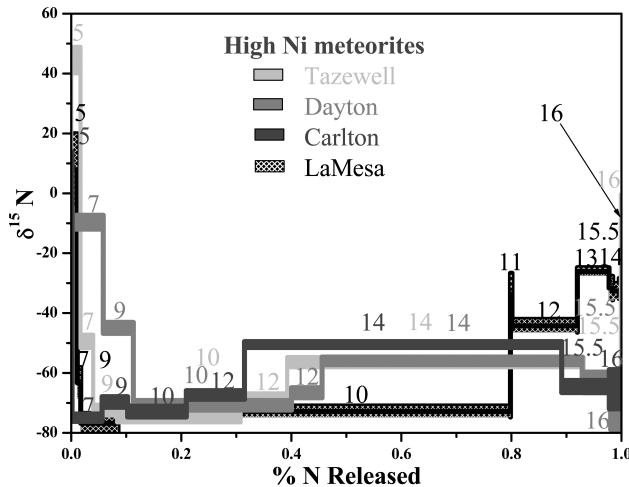


Fig. 2. A comparison of high-Ni meteorites: Carlton, Dayton, Tazewell, and Lamesa. Note that Dayton and Tazewell have nearly identical N step-releases, which suggests an origin from the same parent body. However, the $^{21}\text{Ne}_c$ concentrations are different. (Lavielle, personal communication). Carlton also has a similar release, although its total $\delta^{15}\text{N}$ is heavier. Lamesa has a distinctive N release from the other three.

in order to compare nitrogen isotopic systematics. Figure 5 shows that isotopic systematics is very similar for both groups, and in both plots, the presence of a second heavier component above 1000 °C is evident. The only apparent difference is in the nitrogen release pattern, specifically in the 1200 °C fractions, indicating at least two resolved major release peaks at 1000 °C and at 1400 °C for the IIICD group, while the IABs show significant gas releases at 1200 °C. However, variations in release patterns may at least in part be due to structural differences between classes.

A Multicomponent Model

It is already clear that the nitrogen data from the metal matrix require more than a single reservoir of N. First, there is a significant light nitrogen reservoir released at low temperature (i.e., ≤ 1000 °C) in most of the samples in this study. In some samples the light signature appears early, as in Carlton, where $\delta^{15}\text{N}$ is already -75‰ at 700 °C, and in Bischtübe 2, where $\delta^{15}\text{N} = -61\text{‰}$ at 700 °C. In Copiapo 2 (Fig. 1), there are two distinct light reservoirs seen; one releases at about 920 °C and the other at 1050 °C. The release step at 900 °C possibly carries a slightly lighter component ($\delta^{15}\text{N} = -82.4\text{‰}$) than the 1050 °C release, but the earlier release might be lighter because of some fractionation in the release. The second N component is very clear, with a peak release at 1050 °C ($\delta^{15}\text{N}$ signature of $-75\text{‰} \pm 2\text{‰}$). We know from previous experiments in our lab that separated troilite releases most of its gases by pyrolysis between 1050 °C to 1100 °C (Murty and Marti 1987; Mathew, personal communication). The high-temperature Xe ratios might

therefore link a N carrier to troilite. In fact, Prombo and Clayton (1993) measured the bulk N signature of troilite ($\delta^{15}\text{N} = -73.2\text{‰} \pm 0.4\text{‰}$) from Canyon Diablo, which is consistent with this signature. However, the large sample of troilite used in that study may have also been affected by inclusions in the troilite. We earlier discussed that the high-temperature Xe data also indicate the presence of some troilite, but cosmic-ray effects are secondary, produced in situ during space exposure. It is not clear that troilite as a secondary phase can retain primitive N components. Graphite is a known carrier of N and can have a number of $\delta^{15}\text{N}$ signatures. (Zipfel et al. 1996) In order to test whether oxidation of graphite embedded in silicates releases N, we did a combustion step at 750 °C in Odessa 5, but no significant release was observed.

Not all samples have this light N in the steps ≤ 1000 °C. Yardymly 3, for example, has a positive $\delta^{15}\text{N}$ up to and including the 1000 °C step. Odessa 5 also lacks a large amount of the light, low-temperature N, as does Bischtübe 1 for steps ≤ 900 °C. There is evidence of a small, low-temperature (i.e., ≤ 700 °C), heavy component of N that might be distinct from fractionated air, but because of its early release, it is difficult to be definitive about its existence. This low-temperature component is seen in Hope, in both samples of Bischtübe, and in Balfour Downs 2 at 500 °C and 700 °C. This labile component persists to 1000 °C in the case of Yardymly, or to 850 °C in the case of Odessa 5.

A heavy nitrogen component is released at high temperature (i.e., >1000 °C) and some of the samples are dominated by a high-temperature release. Even in release patterns dominated by light N, there is generally a dent, usually at about 1400 °C, indicating the existence of a heavy component. This heavy nitrogen probably differs from the low-temperature component unless the release of a single heavy component starts at 500 °C and continues until to 1400 °C. Note that about half of the samples have a lighter signature at 1550 °C, relative to 1400 °C, which precludes a diffusion-fractionated residue due to incomplete extraction as an explanation of these heavier components. Even in a sample dominated by light N, like Copiapo 2, the $\delta^{15}\text{N}$ signature becomes progressively heavier until the 1550 °C extraction step, where it becomes lighter again. We can constrain the signature of heavy N responsible for the “dents,” to $\delta^{15}\text{N} \geq -16\text{‰}$ from the data obtained at 1400 °C for Balfour Downs 2, Odessa 5, and Yardymly 3.

The existence of multiple, distinct reservoirs, whether native to the metal or to some inclusion, demonstrates a lack of isotopic equilibration. We can not exclude the possibility that distinct or changing temporary reservoirs existed on the parent body and that N as a gas was incorporated. Although the formation of the heavier residual reservoirs by large-scale loss mechanisms from the parent body cannot be ignored, nitrogen imports from adjacent phases (e.g., silicates carrying heavy nitrogen) and partial equilibration remain as possible

Table 2. Xe in samples 500–1600 °C.

Meteorite	Temperature (°C)	Concentration of $^{132}\text{Xe}^a$	$^{131}\text{Xe}/^{132}\text{Xe}$	$^{129}\text{Xe}/^{132}\text{Xe}$
Balfour Downs 1	500–1000	1.42 ± 0.14	0.91 ± 0.06	1.25 ± 0.06
	1000–1600	Not detectable	Not detectable	Not detectable
Balfour Downs 2	500–1000	1.05 ± 0.13	0.80 ± 0.12	1.34 ± 0.18
	1000–1600	1.84 ± 0.06	1.10 ± 0.05	1.75 ± 0.08
Bischtübe 1	500–1000	1.15 ± 0.20	0.99 ± 0.06	1.27 ± 0.08
	1000–1600	0.95 ± 0.25	1.07 ± 0.06	2.02 ± 0.14
Bischtübe 2	500–1000	2.04 ± 0.22	0.90 ± 0.25	1.59 ± 0.16
	1000–1600	4.01 ± 0.11	0.92 ± 0.04	1.51 ± 0.04
Carlton	500–1000	Not detectable	Not detectable	Not detectable
	1000–1600	3.69 ± 0.22	1.07 ± 0.20	0.98 ± 0.09
Copiapo 1	500–1000	0.65 ± 0.18	1.23 ± 0.11	1.55 ± 0.11
	1000–1600	1.10 ± 0.11	1.03 ± 0.07	1.59 ± 0.11
Copiapo 2	500–1000	1.81 ± 0.08	0.92 ± 0.07	1.55 ± 0.09
	1000–1600	1.83 ± 0.19	0.88 ± 0.04	1.48 ± 0.07
Dayton	500–1000	1.29 ± 0.09	1.02 ± 0.06	1.25 ± 0.06
	1000–1600	3.79 ± 0.13	0.82 ± 0.03	1.12 ± 0.03
Haniet el Beguel	500–1000	1.37 ± 0.21	1.12 ± 0.10	1.51 ± 0.14
	1000–1600	2.23 ± 0.28	1.08 ± 0.06	1.62 ± 0.10
Hope	500–1000	1.91 ± 0.18	1.06 ± 0.07	1.21 ± 0.13
	1000–1600	0.65 ± 0.24	1.17 ± 0.11	1.31 ± 0.22
Lamesa	500–1000	1.63 ± 0.19	0.91 ± 0.17	1.16 ± 0.25
	1000–1600	1.56 ± 0.17	0.92 ± 0.05	1.70 ± 0.06
Odessa 2	1000–1600	7.28 ± 1.2	0.92 ± 0.04	1.21 ± 0.04
Odessa 4	500–700	1.28 ± 0.12	0.89 ± 0.04	1.15 ± 0.05
	700–1000	1.92 ± 0.11	0.84 ± 0.03	1.16 ± 0.04
	1000–1600	12.8 ± 0.43	0.83 ± 0.02	1.05 ± 0.03
Odessa 5	500–1000	3.79 ± 0.32	0.93 ± 0.06	1.25 ± 0.08
	700 °C combustion	0.40 ± 0.12	1.64 ± 0.16	0.89 ± 0.35
	1000–1600	Not detectable	Not detectable	Not detectable
Sarepta	500–1000	1.08 ± 0.15	0.98 ± 0.07	1.35 ± 0.08
	1000–1600	0.75 ± 0.15	1.10 ± 0.08	1.41 ± 0.08
Tazewell	500–1000	1.51 ± 0.10	0.92 ± 0.05	1.23 ± 0.06
	1000–1600	Not detectable	Not detectable	Not detectable
Yardmyly 3	500–1000	0.65 ± 0.13	0.95 ± 0.08	1.18 ± 0.10
	1000–1600	1.44 ± 0.15	1.26 ± 0.06	2.24 ± 0.11

^aThe Xe data is uncorrected for blanks, but is corrected for mass discrimination and uncertainties in the ratio represent 95% confidence limits. In both the low- and high-temperature ranges, Xe blanks for most of the pyrolysis steps (20 out of 34) were below the detection limit of the mass spectrometer. Ten blanks contained trace amounts of air. The remaining four blanks had small amounts Xe with a signature different from air. These four Xe blanks are consistent with contributions from cosmic-ray reactions on heavy metals (possibly memory from previous samples) and do not fall on the Te(n, γ) line. The ^{132}Xe concentrations are reported in $10^{-12} \times \text{cm}^3$ STP per g.

sources. As discussed earlier, Franchi et al. (1993) did not observe distinct isotopic N components in acid residues. Several authors (e.g., Bogard et al. 1968) have already shown that inclusions such as silicates found in IAB irons carry nearly pristine, heavy, chondritic noble gas compositions. These authors suggest that the trapped ^{132}Xe found in the silicates of IAB irons, like Copiapo, were sealed in slowly

cooling, molten Fe-Ni, which prevented the Xe from degassing. It is reasonable to suggest that one or more N reservoirs survived the IAB iron formation step, as well. The N reservoirs are also heterogeneously distributed, which is consistent with a poorly mixed formation. It seems that a limited amount of isotopic exchange has occurred after the injection of the original sources.

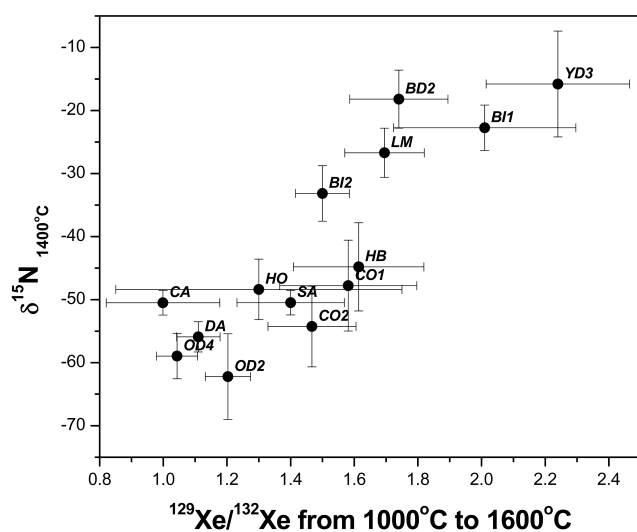


Fig. 3. A plot of $\delta^{15}\text{N}$ at 1400 °C versus $^{129}\text{Xe}/^{132}\text{Xe}$ for the high-temperature steps (1000 °C to 1600 °C). Since amounts of Xe in metal are low, excesses indicate that the metal samples are not free from inclusions. This inclusions are contributing to the total N signature as seen by the correlation between $\delta^{15}\text{N}$ and the Xe ratios. Abbreviations: BD = Balfour Downs, BI = Bischtübe, CA = Carlton, CO = Copiapo, DA = Dayton, HB = Haniet el Beguel, HO = Hope, LM = LaMesa, OD = Odessa, SA = Sarepta, TA = Tazewell, and YD = Yarydmyly.

Nitrogen Reservoirs

A uniform, indigenous nitrogen isotopic signature has been observed in meteoritic and lunar silicates (Mathew and Marti 2001), which contrasts with the variable signatures in metal-rich parent objects. The possibility of an interstellar origin was suggested for the light nitrogen in Acapulco graphite (El Goresy et al. 1995) and for light N signatures in metals of unequilibrated chondrites (Hashizume and Sugiura 1997; Mathew et al. 2005). Heavy N-carriers, such as those found in meteorites like Bencubbin, might also have survived from presolar sources (Franchi et al. 1986). Cr- and Ti-sulfides, produced with extremely large $\delta^{15}\text{N}$ in a supernova or in the silicon-burning stage of a star, were suggested by Franchi et al. (1986). Alternatively, the light nitrogen components may indicate that a light nitrogen signature existed in the primitive solar nebula. On the basis of light nitrogen systematics observed in lunar grains, Hashizumi et al. (2000) proposed the possibility of a very light nitrogen signature in the solar wind. Solar nitrogen was collected during the Genesis mission and plans exist to determine the isotopic abundances.

Nitrogen in irons is not unique in retaining its presumed presolar signatures. Carbon has also been documented to retain many of its primitive signatures. Examples of a refractory carrier with presolar light nitrogen and a distinct carbon isotopic signature have been observed in cohenite and graphite of IAB irons (Deines and Wickman 1975) and can be

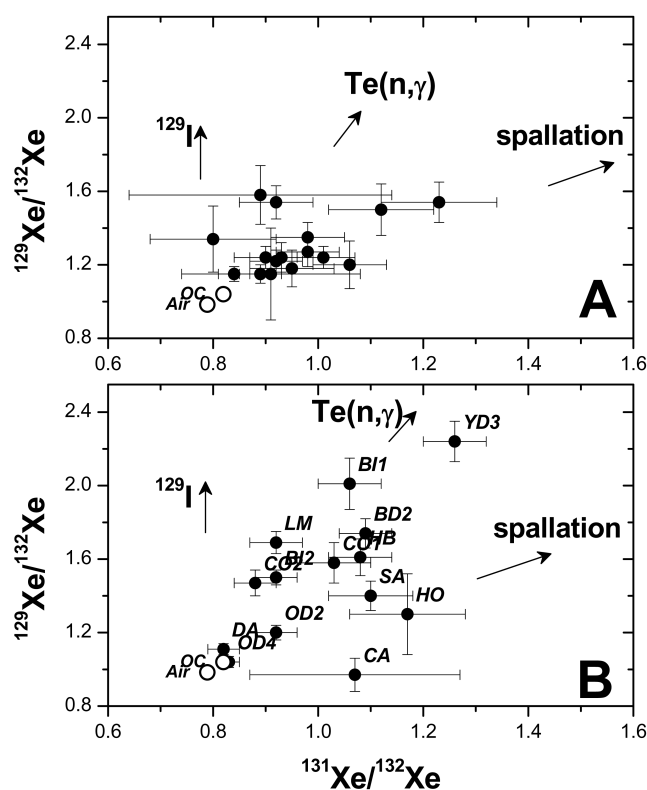


Fig. 4. $^{129}\text{Xe}/^{132}\text{Xe}$ versus $^{131}\text{Xe}/^{132}\text{Xe}$. The abbreviations for the meteorites are as described in Fig. 3. a) In the low-temperature steps (500 °C to 1000 °C), most Xe isotope ratios show small spallation components. b) In the high-temperature steps (1000 °C to 1600 °C), shifts due to $\text{Te}(n,\gamma)$ reactions by epithermal neutrons have a slope of 3.6, suggesting the presence of troilite. (Hwaung and Manuel 1982; Murty and Marti 1987) Also indicated on the plots are shifts in the direction of ^{129}I decay and in the direction for cosmic-ray produced Xe.

found in the form of nanodiamonds or of mainstream SiC. Nitrogen in mainstream SiC grains is highly variable (Hoppe and Ott 1997), but most of the studied grains have $^{12}\text{C}/^{13}\text{C}$ ratios in the range 40–80 and $^{14}\text{N}/^{15}\text{N}$ ratios in the range 500–5000. Isotopic signatures observed in SiC are difficult to explain by processes in the interstellar medium and suggest a circumstellar origin (Hoppe and Ott 1997). The large variations in oxygen isotopic systematics in solar system materials also suggest the survival of a presolar molecular cloud parent (Yurimoto and Kuramoto 2004). According to this model, materials with anomalous isotopic compositions were transported into the solar nebula by icy dust grains during the collapse of the cloud and subsequently evaporated in the inner solar disk. If oxygen in H_2O and CO, the major carriers, were isotopically distinct because of selective UV dissociation of molecules as a result of self-shielding in the cloud, nitrogen-bearing molecules should be affected also.

A number of metals retain their primitive signatures in meteorites. Silver is a volatile element that retains its early isotopic composition. In particular, Ag records the decay

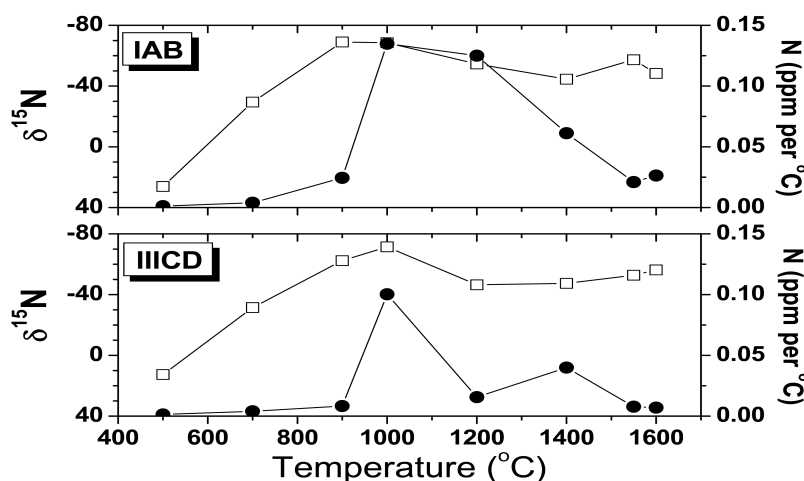


Fig. 5. The weighted average of the N release from the IAB iron group compared to that of the IIICD group. The N released is normalized to ppm per °C. Note that the N systematics are similar except in the 1200 °C step. In IIICD meteorites, the light reservoir is better resolved from high-temperature, heavy reservoir. Both show an early heavy nitrogen release, which signals a labile N component.

products of extinct ^{107}Pd . When ^{107}Ag was studied in metal and troilite of the IAB Canyon Diablo (Carlson and Hauri 2001; Woodland et al. 2005), the data of two studies gave different sulfide segregation times. Woodland et al. (2005) suggest that these data are unlikely to give chronometric information because $\delta^{107}\text{Ag}$ may reflect heterogeneities resulting from variable mixing of the impactor and parent body regolith. Nickel isotopes have been found to have distinct signatures within IAB iron meteorites, as well. Quitté et al. (2006) found distinct ^{60}Ni and ^{61}Ni isotopic variations in two sulfide separates from Odessa and from Toluca, even though the isotopic compositions of the Ni in the metal matrix were indistinguishable from that of the standard. Recently, work has been done on the Tl isotopic variations in irons (Nielsen et al. 2006). The authors have reported distinct variations in the Tl composition between metal and troilite in IAB irons.

History and Isotopic Systematics

As can be seen in the previous discussion, a number of elements with various volatilities retain records of their past history. The formation age record of IAB irons is complex. Bogard et al. (2005) conclude that I-Xe ages reported for some IABs define older ages (4558–4566 Myr), which cannot be easily reconciled with apparently much younger Ar-Ar and Sm-Nd ages. These authors suggest several options to account for the discrepancies: a) higher closure temperatures for Xe did not reset I-Xe ages, b) a bias in the ^{40}K decay constants exists, c) there are uncertainties in reported Sm-Nd and Rb-Sr ages, and/or d) metamorphism has reset the Ar-Ar ages about 30 Myr after the initial differentiation of Caddo silicates and their mixing with metal.

A delayed reheating stage to metamorphic temperatures was also suggested for the parent object of eucrites (possibly

Vesta) based on Hf-W isotopic systematics (Kleine et al. 2005). Since there is an uncertainty in the ^{40}K half-life—49 Myr (Lee 2002) in a 4.56 Gyr old sample—age differences are within experimental uncertainty. The problem with the ^{40}K decay constant was documented by U,Th- ^4He ages for Acapulco apatites (Min et al. 2003). Therefore, the oldest ^{39}Ar - ^{40}Ar ages overlap with a reported ^{147}Sm - ^{143}Nd isochron age for Caddo County silicates (Stewart et al. 1996), and possibly also with the ^{129}I - ^{129}Xe ages of IAB silicates (Niemeyer 1979b).

Exposure histories of iron meteorites are sometimes complex. Because of their hardness, it is generally expected that irons survive on average longer in space than other meteorites. For example, Yardymly has a very long and complex exposure history, as documented by ^{40}K - ^{41}K data (Lavielle et al. 1999). However, a number of the studied main group IAB irons (IAB-MG group) have very low ^{21}Ne concentrations, i.e., $<0.5 \times 10^{-8}$ cm 3 STP/g (Lavielle, personal communication), which implies that the exposure ages are unusually short for irons. How does this relate to the N reservoirs observed in the metal? Most of the IAB/IIICD irons studied show isotopic characteristics of heavier N at 1400 °C because of an increase in the relative contribution of the high-temperature, heavy component. Interestingly, Yardymly is one of the exceptions. Has the release systematics been affected by a postformation collision during its exposure history?

Nitrogen Gain/Loss Mechanisms and Origin

As was discussed previously, there are several irons displaying light N release at the 900 °C and the 1000 °C steps. We see at least one light N component released in Copiapo between 700 °C and 900 °C (see Fig. 1) with a $\delta^{15}\text{N}$ signature of $-82 \pm 2\%$. In addition, we measured a few acid-etched

samples (not discussed here) that released the light nitrogen component at even lower temperatures (≤ 700 °C) than in the unetched samples. Acid etching may open up diffusion channels in the metal matrix, which might allow the trapped nitrogen to be extracted sooner. Early N release might occur because of phase or compositional changes. Labile structures are known in irons. Yang et al. (1997) studied low-temperature phase decomposition in metal and observed complex phase transformations at ≤ 400 °C. Nitrogen carriers, incorporated into the metastable phases during their cooling history, may be expected to expel gases during phase transitions in the step-heating mode. The unstable microstructures may develop when Fe-Ni metal is cooled during metamorphism or by shock events. Yang et al. (1997) discussed the “cloudy zone” which develops by decomposition below 350 °C and the metastable island regions of high Ni content and metastable honeycomb regions of low Ni content that are formed at these low temperatures.

We also note that Tong et al. (2003) found that the formation of nitrides from gas phase nitrogen in a nanostructured surface layer is greatly enhanced. These authors find that the nitriding temperatures can be as low as 300 °C in a plastic deformation zone such as induced by an impacting sphere. Another experiment shows that the nitrogen distributions in hot implanted Fe and Fe-Ti films indicate a redistribution mechanism in metal surfaces (Ohtani et al. 1997). These authors observe that during the irradiation of Fe with 300 keV N_2^+ ions, iron nitrides (Fe_2N , Fe_4N) are found at surface temperatures of 350° and 500 °C. In Fe-Ti alloy films at 350 °C, they also observed a diffraction ring corresponding to TiN and Fe_3N , and at 500 °C, TiN was prominent. These authors infer that at 500 °C many dispersed particles of TiN of 10–50 nm can be formed, and that in their experiment nitrogen atoms were initially bound to Fe and Ti during the implantation, but that apparently iron nitrides decomposed and that N diffused in the iron lattice to form TiN which in turn may precipitate. We suppose that if moveable nitrogen atoms can be fixed in nitrides, such as CrN or TiN, this may represent a possible mechanism of nitrogen incorporation and for the formation of nitrides (Ponganis et al. 2000). In light of a complex cooling history, a redistribution of nitrogen into metastable phases might explain the relatively early nitrogen releases. Hashizume and Sugiura (1997) estimated a closure temperature of ≤ 500 °C for nitrogen dissolved in taenite in a slowly cooling body with a nitrogen concentration of ~ 10 ppm nitrogen in the taenite when the metal was in equilibrium with nitrogen gas at 500 °C and 1 bar pressure.

We infer from the IAB iron nitrogen data that the light N was processed locally and did not equilibrate. At least one light N component survived the formation processes of iron parent objects. Observed interplanetary dust particles with anomalous nitrogen may have their origin in the interstellar medium (Floss et al. 2006), but also processed meteorites

carry organic matter with primitive nitrogen isotopic signatures (Busemann et al. 2006), which imply their preservation in the asteroid belt and in the early solar nebula. The preservation of distinct N signatures extends trends observed in primitive achondrites. This supports models that light nitrogen was carried by presolar grains, and following their incorporation into IAB parent object(s), was transferred to the metal without exchanging, or only partially exchanging, with nitrogen in other phases, such as silicates.

Evidence for incomplete mixing of nucleosynthetic components was first observed in Sm isotopes of a CAI in Allende (Lugmair et al. 1978). The carbon and nitrogen isotopic signatures in the Acapulco meteorite have a large range of values (El Goresy et al. 1995). Mo and Ru isotopic systematics of iron meteorites is complex (Dauphas et al. 2004). The Mo and Ru anomalies in iron meteorites appear to be correlated with nucleosynthetic processes. Isotopic variations of Mo and Ru document an incomplete homogenization for solar system of s-process products (Dauphas et al. 2004). The nuclear signature of the s-process is produced in low-mass AGB stars. Since irons of different groups show variable shifts in Mo and Ru isotopic signatures, Dauphas et al. (2004) suggest that different regions of the nebula received variable inputs of s-process matter. Incomplete equilibration is also suggested for the Hf-W systematics in differentiated eucrites (Kleine et al. 2005). How can the formation of iron parent bodies be coupled to presolar carrier materials? It is possible that early average accretionary matter had an s-process deficit, and was not homogenized as documented by variable s-process deficits observed in iron meteorites. The nitrogen concentrations in mainstream SiC grains are high (percent level [Hoppe and Ott 1997]). Therefore, the nitrogen budgets may be accounted for by small amounts of carriers. Nevertheless, a transfer mechanism to irons on their differentiated parent objects is still required and places constraints on the evolutionary histories. Heat pulses generated in collisional events (Woodland et al. 2005) may have played an important role in parent body evolution. Such events might also account for the distinct isotopic signature carried by impactors. If cooling occurs rapidly, incorporated carriers would be able to retain the signatures of trapped components and escape significant isotopic exchange.

SUMMARY AND CONCLUSIONS

We studied and discussed nitrogen isotopic signatures as observed by stepwise pyrolysis in 17 samples of 12 IAB/IIICD iron meteorites. The data lead to the following observations and conclusions:

1. Nitrogen isotopic analysis of iron meteorites by the method of stepwise pyrolysis at increasing temperatures permits the resolution of indigenous, distinct and heterogeneously distributed nitrogen components. At

least two light, low-temperature N reservoirs exist and at least one, and maybe several, heavy reservoirs as well.

2. We discussed some possible sources and incorporation and transfer mechanisms to preserve the heterogeneous nitrogen components. These factors constrain not only the formation and cooling history, but also metamorphic events. For example, heat pulses due to collisional events. As suggested by Wasson and Kallemeyn (2002), Choi et al. (1995), and Woodland et al. (2005), may satisfy such constraints. We note that Kleine et al. (2005) recently suggested that impact events might have facilitated the thermal metamorphism of eucrites, based on observed radiogenic W in the metal.
3. The observed distinct indigenous nitrogen components suggest different origins for the light and heavy nitrogen signatures and suggest that nonmagmatic iron parent objects formed without full equilibration of their nitrogen reservoirs. The data can be constrained to possibly two major reservoirs with a limited amount of isotopic exchange.
4. The high-Ni IIICD irons Carlton, Dayton, and Tazewell show very similar release patterns and light N isotopic signatures. The data for these meteorites are consistent with our IAB irons, unlike their molybdenum signatures, which do not substantiate a link (Dauphas et al. 2002).
5. Noble gas isotopic signatures, specifically of Xe, represent useful indicators for the presence of minor amounts of contaminating minerals because the metal matrix contains very low concentrations of indigenous Xe. Correlated releases of excess ^{129}Xe and ^{131}Xe in several of the irons are indicative of epithermal neutron reactions on Te and may indicate the presence of troilite inclusions.

Acknowledgments—We thank Bernard Lavielle for communicating unpublished CRE Ne data of irons. Candace Kohl helped with tests using acid treatments, and K. J. Mathew is thanked for several discussions. We acknowledge many useful comments by reviewers Bernard Marty, Richard Becker, and Associate Editor Ian Franchi. This research was supported by NASA grants NAG5-12983 and NNG05GJ08G.

Editorial Handling—Dr. Ian Franchi

REFERENCES

- Benedix G. K., Lauretta D. S., and McCoy T. J. 2005. Thermodynamic constraints on the formation conditions of winonaites and silicate-bearing IAB irons. *Geochimica et Cosmochimica Acta* 69:5123–5131.
- Bogard D., Burnett D. S., Eberhardt P., and Wasserbury G. J. 1968. ^{40}Ar - ^{40}K ages of silicate inclusions in iron meteorites. *Earth and Planetary Science Letters* 3:275–283.
- Bogard D. D., Garrison D. H., and Takeda H. 2005. Ar-Ar and I-Xe ages and the thermal history of IAB meteorites. *Meteoritics & Planetary Science* 40:207–224.
- Buchwald V. F. and Scott E. R. D. 1971. First nitride (CrN) in iron meteorites. *Nature* 233:113–14.
- Busemann H., Young A. F., Alexander C. M. O'D., Hoppe P., Mukhopadhyay S., and Nittler L. R. 2006. Interstellar chemistry recorded in organic matter from primitive meteorites. *Science* 312:727–730.
- Carlson R. W. and Hauri E. H. 2001. Extending the Pd-107-Ag-107 chronometer to low Pd/Ag meteorites with multicollector plasma-ionization mass spectrometry. *Geochimica et Cosmochimica Acta* 65:1839–1848.
- Choi B. G., Ouyang X. W., and Wasson J. T. 1995. Classification and origin of IAB and IIICD iron meteorites. *Geochimica et Cosmochimica Acta* 59:593–612.
- Dauphas N., Davis A. M., Bernard M., and Reisberg L. 2004. The cosmic molybdenum-ruthenium isotope correlation. *Earth and Planetary Science Letters* 226:465–475.
- Dauphas N., Marty B., and Reisberg L. 2002. Molybdenum evidence for inherited planetary scale isotope heterogeneity of the protosolar nebula. *The Astrophysical Journal* 565:640–644.
- Deines P. and Wickman F. E. 1975. A contribution to the stable carbon isotope geochemistry of iron meteorites. *Geochimica et Cosmochimica Acta* 39:547–557.
- El Goresy A., Zinner E., and Marti K. 1995. Survival of isotopically heterogeneous graphite in a differentiated meteorite. *Nature* 373:496–499.
- Floss C., Stadermann F. J., Bradley J. P., Dai Z. R., Bajt S., Graham G., and Lea A. S. 2006. Identification of isotopically primitive interplanetary dust particles: A nanoSIMS isotopic imaging study. *Geochimica et Cosmochimica Acta* 70:2371–2399.
- Franchi I. A., Wright I. P., and Pillinger C. T. 1986. Heavy nitrogen in Bencubbin—A light-element isotopic anomaly in a stony-iron meteorite. *Nature* 323:138–140.
- Franchi I. A., Wright I. P., and Pillinger C. T. 1993. Constraints on the formation conditions of iron meteorites based on concentrations and isotopic compositions of nitrogen. *Geochimica et Cosmochimica Acta* 57:3105–21.
- Goldstein J. I. and Ogilvie R. E. 1965. Growth of Widmanstätten pattern in metallic meteorites. *Geochimica et Cosmochimica Acta* 29:893–896.
- Hashizume K. and Sugiura N. 1997. Isotopically anomalous nitrogen in H-chondrite metal. *Geochimica et Cosmochimica Acta* 61:859–872.
- Hashizume K., Chaussidon M., Marty B., and Robert F. 2006. Solar wind record on the moon: Deciphering presolar from planetary nitrogen. *Science* 290:1142–1145.
- Herpfer M. A., Larimer J. W., and Goldstein J. I. 1994. A comparison of metallographic cooling rate methods used in meteorites. *Geochimica et Cosmochimica Acta* 58:1353–1365.
- Hopfe W. D. and Goldstein J. I. 2001. The metallographic cooling rate method revised: Application to iron meteorites and mesosiderites. *Meteoritics & Planetary Science* 36:135–154.
- Hoppe P. and Ott U. 1997. Mainstream silicon carbide grains from meteorites. In *Astrophysical implications of the laboratory study of presolar materials*, edited by Bernatowicz T. J. and Zinner E. K. Woodbury, New York: The American Institute of Physics. pp. 27–58.
- Horan M. F., Smoliar M. I., and Walker R. J. 1998. W-182 and Re-187-Os-187 systematics of iron meteorites: Chronology for melting, differentiation, and crystallization in asteroids. *Geochimica et Cosmochimica Acta* 62:545–554.
- Hwaung G. and Manuel O. K. 1982. Terrestrial-type xenon in meteoritic troilite. *Nature* 299:807–810.
- Kelly W. R. and Larimer J. W. 1977. Chemical fractionations in

- meteorites. VIII. Iron meteorites and the cosmochemical history of the metal phase. *Geochimica et Cosmochimica Acta* 41:93–111.
- Kleine T., Mezger K., Palme H., Scherer E., and Munker C. 2005. Early core formation in asteroids and late accretion of chondrite parent bodies: Evidence from Hf-182-W-182 in CAIs, metal-rich chondrites, and iron meteorites. *Geochimica et Cosmochimica Acta* 69:5805–5818.
- Lavielle B., Marti K., Jeannot J. P., Nishiizumi K., and Caffee M. 1999. The Cl-36-Ar-36-K-40-K-41 records and cosmic ray production rates in iron meteorites. *Earth and Planetary Science Letters* 170:93–104.
- Lee J. K. W. 2002. Decay-constant uncertainties of K-40 and the Ar-40/Ar-39 age equation. *Geochimica et Cosmochimica Acta* 66: A444–A444.
- Lugmair G. W., Marti K., and Scheinin N. B. 1978. Incomplete mixing of products from r-, p-, and s-process nucleosynthesis: Sm-Nd systematics in Allende inclusion EK 1-04-1. Proceedings, 9th Lunar Science Conference. pp. 672–674.
- Markowski A., Quitté G., Halliday A. N., and Kleine T. 2006. Tungsten isotopic compositions of iron meteorites: Chronological constraints versus cosmogenic effects. *Earth and Planetary Science Letters* 242:1–15.
- Maruoka T., Matsuda J., and Kurat G. 2001. Abundance and isotopic composition of noble gases in metal and graphite of the Bohumilitz IAB iron meteorite. *Meteoritics & Planetary Science* 36:597–609.
- Mathew K. J. and Begemann F. 1995. Isotopic composition of xenon and krypton in silicate-graphite inclusions of the El Taco, Campo del Cielo, IAB iron meteorite. *Geochimica et Cosmochimica Acta* 59:4729–46.
- Mathew K. J. and Marti K. 2001. Lunar nitrogen: Indigenous signature and cosmic ray production rate. *Earth and Planetary Science Letters* 184:659–669.
- Mathew K. J., Marti K., and Kim Y. 2005. Nitrogen in chondritic metal. *Geochimica et Cosmochimica Acta* 69:753–762.
- Mathew K. J., Palma R. L., Marti K., and Lavielle B. 2000. Isotopic signatures and origin of nitrogen in IIE and IVA iron meteorites. *Geochimica et Cosmochimica Acta* 64:545–557.
- Meshik A., Kurat G., Pravdivtseva O. V., and Hohenberg C. W. 2004. Radiogenic 129-xenon in silicate inclusions in the Campo del Cielo iron meteorite (abstract #1687). 36th Lunar and Planetary Science. CD-ROM.
- Min K., Farley K. A., Renne P. R., and Marti K. 2003. Single grain (U-Th)/He ages from phosphates in Acapulco meteorite and implications for thermal history. *Earth and Planetary Science Letters* 209:323–336.
- Murty S. V. S. and Marti K. 1987. Nucleogenic noble-gas components in the Cape York iron meteorite. *Geochimica et Cosmochimica Acta* 51:163–172.
- Murty S. V. S. and Marti K. 1994. Nitrogen isotopic signatures in Cape York: Implications for formation of group III A irons. *Geochimica et Cosmochimica Acta* 58:1841–1848.
- Nielsen H. P. and Buchwald V. F. 1981. Roaldite, a new nitride in iron meteorites. Proceedings, 12th Lunar and Planetary Science Conference. pp. 1343–1348.
- Nielsen S. G., Rehkamper M., and Halliday A. N. 2006. Large thallium isotopic variations in iron meteorites and evidence for lead-205 in the early solar system. *Geochimica et Cosmochimica Acta* 70:2643–2657.
- Niemeyer S. 1979a. ⁴⁰Ar-³⁹Ar dating of inclusions from IAB iron meteorites. *Geochimica et Cosmochimica Acta* 43:1829–1840.
- Niemeyer S. 1979b. I-Xe dating of silicate and troilite from IAB iron meteorites. *Geochimica et Cosmochimica Acta* 43:843–860.
- Ohtani S., Inoue M., and Takagi T. 1997. Nitrogen distribution and microstructure of hot implanted Fe-Ti alloy films. *Nuclear Instruments and Methods in Physics Research B* 121:319–322.
- Pepin R. O. and Becker R. H. 1982. Nitrogen isotopes in iron meteorites (abstract). *Meteoritics* 17:269.
- Ponganis K. V., Kohl C. P., and Marti K. 2000. Nitrogen sources in IAB iron meteorites and their implications (abstract #1412). 31st Lunar and Planetary Science Conference. CD-ROM.
- Prombo C. A. and Clayton R. N. 1993. Nitrogen isotopic compositions of iron meteorites. *Geochimica et Cosmochimica Acta* 57:3749–61.
- Quitté G. and Birck J. L. 2004. Tungsten isotopes in eucrites revisited and the initial Hf-182/Hf-180 of the solar system based on iron meteorite data. *Earth and Planetary Science Letters* 222:331–331.
- Quitté G., Meier M., Latkoczy C., Halliday A. N., and Gunther D. 2006. Nickel isotopes in iron meteorites—Nucleosynthetic anomalies in sulphides with no effects in metals and no trace of Fe-60. *Earth and Planetary Science Letters* 242:16–25.
- Schultz T., Münker C., Mezger K., and Palme H. 2006. Age and origin of IAB iron meteorites and their silicate inclusions inferred from Hf/W chronometry (abstract #1401). 37th Lunar and Planetary Science Conference. CD-ROM.
- Stewart B., Papanastassiou D. A., and Wasserburg G. J. 1996. Sm-Nd systematics of a silicate inclusion in the Caddo IAB iron meteorite. *Earth and Planetary Science Letters* 143:1–12.
- Sugiura N. 1998. Ion probe measurements of carbon and nitrogen in iron meteorites. *Meteoritics & Planetary Science* 33:393–409.
- Takeda H., Bogard D. D., Mittlefehldt D. W., and Garrison D. H. 2000. Mineralogy, petrology, chemistry, and Ar-39-Ar-40 and exposure ages of the Caddo County IAB iron: Evidence for early partial melt segregation of a gabbro area rich in plagioclase-diopside. *Geochimica et Cosmochimica Acta* 64:1311–1327.
- Tong W. P., Tao N. R., Wang Z. B., Lu J., and Lu K. 2003. Nitriding iron at lower temperatures. *Science* 299:686–688.
- Voshage H. and Feldmann H. 1979. Investigations on cosmic-ray-produced nuclides in iron-meteorites 3. Exposure ages, meteoroid sizes and sample depths determined by mass-spectrometric analyses of potassium and rare-gases. *Earth and Planetary Science Letters* 45:293–308.
- Wasson J. T. and Kallemeyn G. W. 2002. The IAB iron-meteorite complex: A group, five subgroups, numerous grouplets, closely related, mainly formed by crystal segregation in rapidly cooling melts. *Geochimica et Cosmochimica Acta* 66:2445–2473.
- Woodland S. J., Rehkamper M., Halliday A. N., Lee D. C., Hattendorf B., and Gunther D. 2005. Accurate measurement of silver isotopic compositions in geological materials including low Pd/Ag meteorites. *Geochimica et Cosmochimica Acta* 69: 2153–2163.
- Yang C. W., Williams D. B., and Goldstein J. I. 1997. A new empirical cooling rate indicator for meteorites based on the size of the cloudy zone of the metallic phases. *Meteoritics & Planetary Science* 32:423–429.
- Yurimoto H. and Kuramoto K. 2004. Molecular cloud origin for the oxygen isotope heterogeneity in the solar system. *Science* 305: 1763–1766.
- Zipfel J., Mathew K. J., and Marti K. 1996. Nitrogen isotopic composition of metal and graphite separates from the El Taco (IAB) iron meteorite (abstract). 27th Lunar and Planetary Conference. pp. 1501–1502.